

Behaviour of steel moment connections with a single flange rib

Cheng-Chih Chen ^{*}, Jen-Ming Lee, Ming-Chih Lin

Department of Civil Engineering, National Chiao Tung University, Hsinchu 30010, Taiwan

Received 22 June 2002; received in revised form 10 April 2003; accepted 14 April 2003

Abstract

This paper presents a study of flange rib moment connections for use in steel moment-resisting frames. The connections are strengthened by welding a vertical rib to the beam flange and the column flange. The rib is characterized by an extension. Finite element analysis and experiments were conducted to elucidate the behaviour of lengthened rib reinforced connections. The results of the finite element analysis established the effectiveness of the lengthened rib in mitigating local stress concentrations and forming the plastic hinge zone in the beam. Two full-scale proof-test specimens behaved as observed by the analysis, and exhibited greater than 3% radians of plastic rotation under cyclic load. Without brittle fracture, both specimens developed a plastic hinge in the beam. Extensive yielding and local buckling occurred in the beam flanges and the web. The connections strengthened with a single flange rib were successfully verified by the test.

© 2003 Elsevier Ltd. All rights reserved.

Keywords: Connection; Flange rib; Plastic rotation

1. Introduction

Based on the seismic design philosophy for steel moment frames, structures are required to remain elastic during small to medium earthquakes. In a large earthquake, such structures should be ductile and safe from collapse. However, many fractures have been found in the connections of moment-resisting frames shaken during the Northridge earthquake in 1994 [1]. Such fractures were most often initiated at the bottom flange weld and propagated into the column flange and the beam web. The fracture prevents the intended inelastic behaviour of the connections.

Two fan type weld access holes in the beam web near the flange are needed to perform full penetration groove welding between the beam flange and the column flange, as required to form the moment connections. The presence of those weld access holes in the beam web causes stress concentration near the center of the beam flange. Consequently, brittle failure can be caused in the weld access hole region for various reasons, such as the presence of weld defects, residual stress due to welding,

stress concentration, and geometric discontinuity. Miller [2] reported that one type of crack observed in the Northridge earthquake was initiated at the point of intersection between the weld access hole and the beam bottom flange. Nakashima et al. [3] also reported that many fractures observed in beam-to-column welded connections during the 1995 Kobe earthquake occurred in weld metals, heat-affected zones, base metals, and diaphragm plates, mostly located at beam bottom flanges. Fractures in base materials were initiated from the toe of weld access holes.

The fracturing initiated near the weld access hole region has been documented in the laboratory. Lin et al. [4] tested four welded beam-to-column subassemblies constructed with slab and weak panel zone. After the panel zone developed extensive inelastic deformation, three out of four specimens exhibited fracturing in the beam bottom flanges near the web cope.

Since the Northridge earthquake, numerous experimental and analytical studies have been conducted to improve connection performance. Among many connections investigated in the literature, two categories of connections are frequently employed to enhance ductility under severe seismic loads. One of the two categories is the reinforced connections, in which the cover plate or haunch are used to strengthen the connections [5–10].

^{*} Corresponding author. Fax: +886-3-572-7109.
E-mail address: chrischen@mail.nctu.edu.tw (C.-C. Chen).

The other category is the reduced beam section (RBS) connections, also known as the ‘dogbone’ connections [11–16]. In the RBS connections, portions of the beam flange are trimmed to ascertain the occurrence of a plastic hinge. Both types of connections use the strategy of controlling the yielding mechanism at a desirable location on the beam. However, the former is labor intensive and costly, while the later may result in reduction in elastic stiffness of a moment frame [13].

Only very limited test data are available concerning the welded moment connections reinforced by vertical flange rib plates. Specimens and their behaviour are briefly described as follows.

Engelhardt et al. [6] tested two full-scale moment connections reinforced by vertical ribs. Two specimens were fabricated using a W14 × 426 (A572 Grade 50) column and a W36 × 150 (A36) beam. Two tapered ribs were welded to the top and bottom beam flanges to reduce the stress on the beam flange groove welds and move the location of the beam plastic hinge away from the face of the column. The backup bar on the bottom flange of the beam was removed. Test results revealed that both specimens performed very well with maximum beam plastic rotation of 2.5 and 3% radians, and exhibited the same ductile behaviour and failure modes. Failure occurred by gradual tearing of the beam bottom flange at the tips of the ribs. Notably, failure did not occur in the column flange near the welded ribs, since the columns used in the test were very heavy.

Anderson and Duan [17] tested three specimens that a vertical triangular plate (fin) was welded to the top and bottom flanges of the beam. Test results showed that specimens developed capacities for plastic rotation in the range of 2.5–3.0% radians. The specimen having a welded solid fin failed due to the pullout of the top fin from the weld at the face of the column. One of two specimens with a welded perforated fin exhibited severe local buckling of the beam flange and web, and minor cracking in the weld at the toe of the fin. The other specimen failed suddenly because of cracking in the weld between the fin and the column flange, pulling out of the beam bottom flange from the column flange, and the penetration of crack into the column flange and its propagation into the column web.

Zekioglu et al. [18] tested three connections. Their specimens had a reduced beam section, and two triangular rib plates were welded to each beam flange. High beam plastic rotation capacities with considerable flexural strength were obtained. Final failure, identical for all three specimens, was by fracture at the narrowest section of the beam flange. Vertical rib plates helped to reduce stresses of groove welds between the beam flange and the column flange, and no damage was observed in the vertical rib plate.

Results in the above studies have provided much valuable insight into the effectiveness of flange ribs. A flange

rib strengthened connection is proposed herein to eliminate the damage associated with the rib plate, such as fracturing of the beam flange at the rib tip and fracturing of the weld between the rib and the column flange. This study develops a connection strengthened by the lengthened flange rib to ensure stable strength and stiffness, and reliable inelastic behaviour. Analytical and experimental results are used to confirm the behaviour and performance of such a connection.

2. Lengthened flange rib design concept

Previous research, as mentioned above, has used two spaced ribs or a triangular rib on each beam flange in a flange rib connection. The rib plates are intended to reduce the demand on the full penetration weld between the beam flange and the column flange, and move the plastic hinge away from the face of the column.

In this work, a single lengthened rib is designed to be welded to beam and column flanges in the plane of both the beam web and the column web. Fig. 1 illustrates the configuration of the connection strengthened by lengthened ribs. Unlike typical triangular rib plates, the lengthened rib consists of three parts, which are a main reinforced part, a curved part, and an extension. The curved part is intended to provide a smooth transition

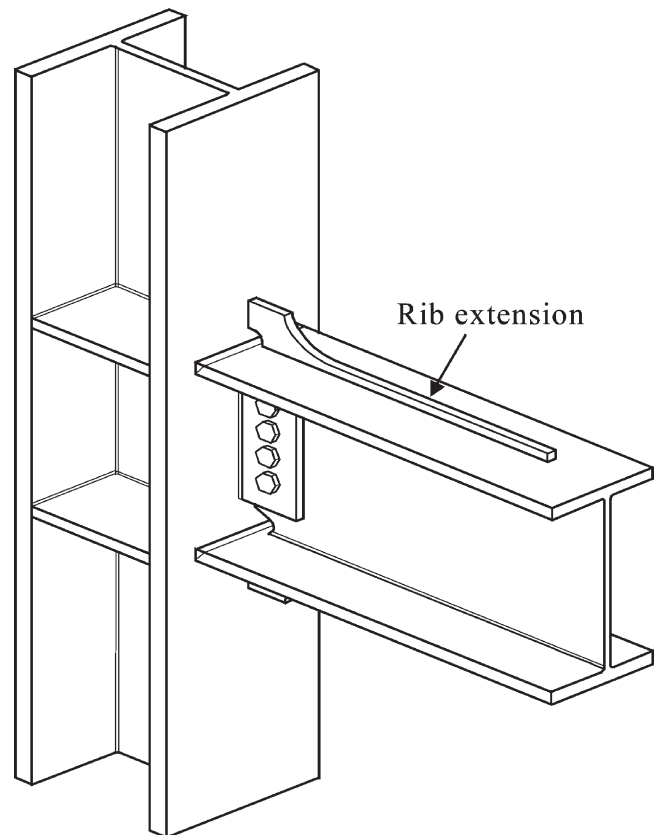


Fig. 1. Lengthened flange rib strengthened connection.

from the main reinforced part of the rib to the rib extension, and to prevent undercutting of the rib plate during manufacture and possible crack initiation.

The single rib plate welded to the plane of the column web enhances the transfer of force to the column, since both rib plate and column web are in the same plane. Apparently, the possible failure of out-of-plane distortion of the column flange caused by two spaced ribs is eliminated.

The rib extension is designed to attenuate the potential stress concentration in the beam flange at the rear end (the end away from the column face) of the triangular rib, and prevent the tearing of the beam flange. The purpose of the rib extension is further to move the plastic hinge of the beam away from the column face, and form the plastic hinge in the beam starting at the front end of the rib extension. The formation of the plastic hinge in the beam leads to large plastic rotations that permit hysteretic dissipation of energy during a severe earthquake. Furthermore, the rib extension creates an extended yielding zone.

Non-linear finite element analysis and full-scale experiments were conducted to examine the performance of connections strengthened by a lengthened rib and thus verify the lengthened rib's effectiveness.

3. Finite element analysis

3.1. Finite element modeling

The general purpose finite element program ANSYS [19] was used for this numerical study. A three-dimensional finite element model was generated to represent a structural subassembly. Fig. 2 presents the finite element mesh. This subassembly was an exterior beam-to-column connection that was isolated from the midheight of two adjacent floor columns and the mid-span of the beam. Only half of the subassembly was modeled because of the symmetry of the model about the plane at the beam web and the column web. The beam was assumed to be a rolled H-shaped steel of $H700 \times 300 \times 13 \times 24$ (dimensions in mm for beam depth, width, web thickness, and flange thickness, respectively), confirmed to ASTM A36 material. The column was assumed to be an $H550 \times 550 \times 36 \times 40$, confirmed to ASTM A572 Gr. 50 material. The lengthened rib was 22 mm thick, 95 mm high, and 700 mm long with a 20 mm high extension. Ignoring the shear tab, the beam web was modeled to be welded directly to the column flange to simplify the modeling. Nevertheless, weld access holes were modeled as closely as possible to identify the nearby stress. Deformation constraints, hinged supports provided at both ends of the column, were assumed to be consistent with the subassembly and the test specimen.

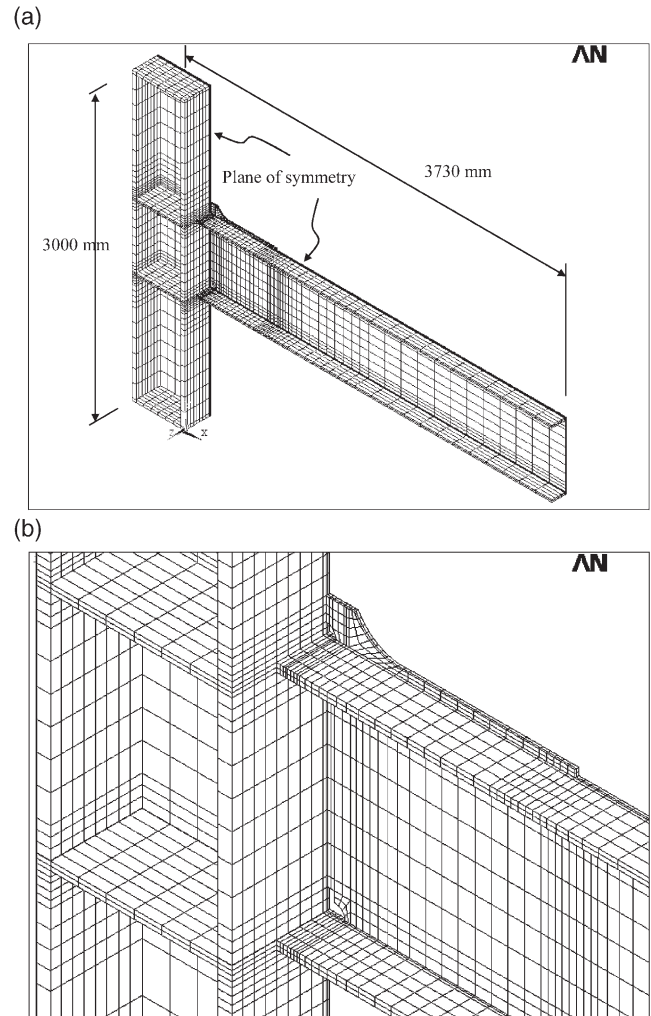


Fig. 2. Three-dimensional finite element mesh.

Brick elements with eight nodes 24 nodal degrees of freedom, three translational DOFs at each node, were used to model the steel shape. The model comprised 4706 elements and 8072 nodes. The yield stresses used to model the beam and the column were 310 and 380 MPa, respectively, to account for the higher actual material strength. The stress-strain relationship for structural steel used in the analysis was modeled as a bilinear relation with linear elastic and strain hardening behaviour. The modulus of elasticity of 200 GPa was assumed for the elastic range and 4% of that was specified for the modulus in the strain hardening range. Von Mises yield criterion and the isotropic hardening rule were employed to define the plasticity. The load was applied by imposing incremental vertical displacements, in a monotonic fashion, at the beam tip during the analysis.

3.2. Analysis results

The analysis results are presented to elucidate the stress distribution, yielding, plastification, and plastic

hinge formation. The results for the interface of the joint and adjacent beam section are emphasized because the subassembly was modeled to have a strong-column weak-beam, and a strong panel zone. Fig. 3 presents stress distribution and the spread of yielding zones at various stages of loading. The figures show the distribution of von Mises stresses as the deflection at the beam tip varied. The Δ_y , shown in the figures, is the calculated deflection at the beam tip when the beam reaches its yield moment.

According to the above figures, the highest stress at each stage was in the weld metal between the rib plate and the column flange, and in the complete joint penetration weld. Notably, however, the strength of the weld metal usually far exceeded that of the structural steel. The yielding of the beam was initiated in the beam flange at the front part of the rib extension. Significant

yielding and plastification of the beam occurred in the beam flanges and the beam web within the rib extension. It was also evident that no sign of the development of high stresses was found near weld access holes. No localized high stress concentration was observed in the beam flange at the rear end of the rib because of the effect of the rib extension. These observations clearly indicate that lengthening the rib leads to the formation of the plastic hinge in the beam section away from the column face. The energy dissipated within the beam section is deemed to be more reliable than that dissipated starting from the face of the column.

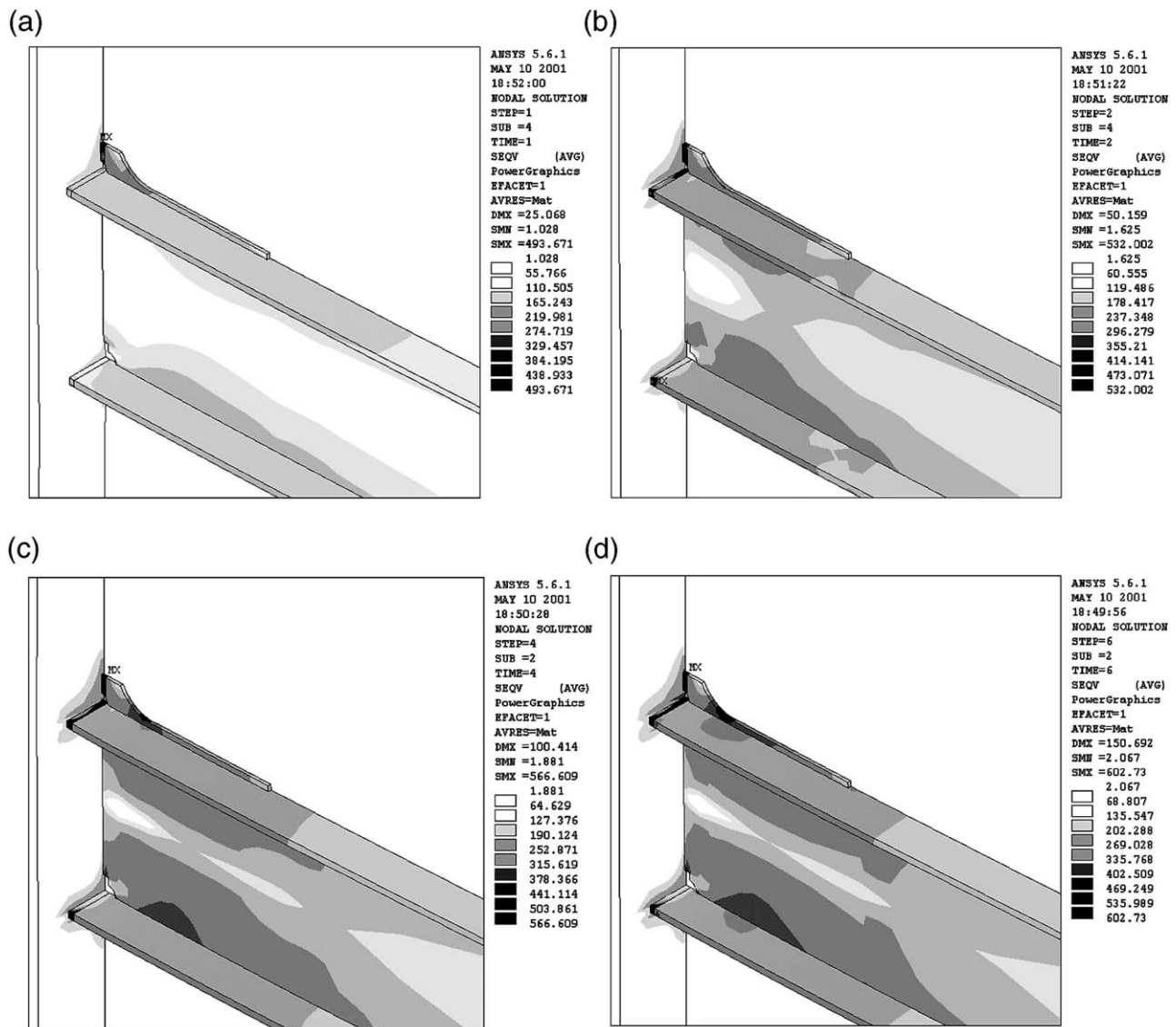


Fig. 3. Von Mises stresses distribution at various beam tip displacements.

Table 1
Specimen designation

Specimen	Beam size ^a	Column size ^a	Rib size
SRL30	H588 × 300 × 12 × 20 A36	H550 × 550 × 30 × 40 A572 Gr. 50	PL30 × 125 × 800 A572 Gr. 50
SRL20	H588 × 300 × 12 × 20 A36	H550 × 550 × 32 × 40 A572 Gr. 50	PL20 × 125 × 800 A572 Gr. 50

^a Rolled H-section whose dimensions are the depth, width, web thickness, and flange thickness (in mm) of the section, respectively.

4. Experimental program

4.1. Test specimens and materials

An experiment was conducted to verify the behaviour of moment connections reinforced by the lengthened flange rib. Specimens represented a structural sub-assembly isolated from the inflection points of a structure. Two exterior, T-shaped beam-to-column connections were designed with a vertical lengthened rib plate, as described in the analytical model. Table 1 details the specimens. Both specimens had the same rolled shape beam. The shape of the beam is much close to the W24 × 104 structural shape used in the US. [20]. Although a smaller and shorter beam, compared with that modeled in the finite element analysis, was used for the test specimens, this experiment was performed to study the behaviour qualitatively. Table 2 lists material properties of the specimens obtained in coupon tests. It is noted that the yield stresses used in the finite element analysis are approximately equal to the average values of actual yield stresses of the flange and the web.

Fig. 4 depicts the connection details. Both specimens had a rib 125 mm maximum high and 800 mm long. The height of the rib was limited to be less than the thickness of the concrete slab. The length of the rib extension was chosen to be equal to the depth of the beam. Specimen SRL30 used a 30 mm thick rib with a 30 mm high rib extension while specimen SRL20, less reinforced, used a 20 mm thick plate and a 20 mm high

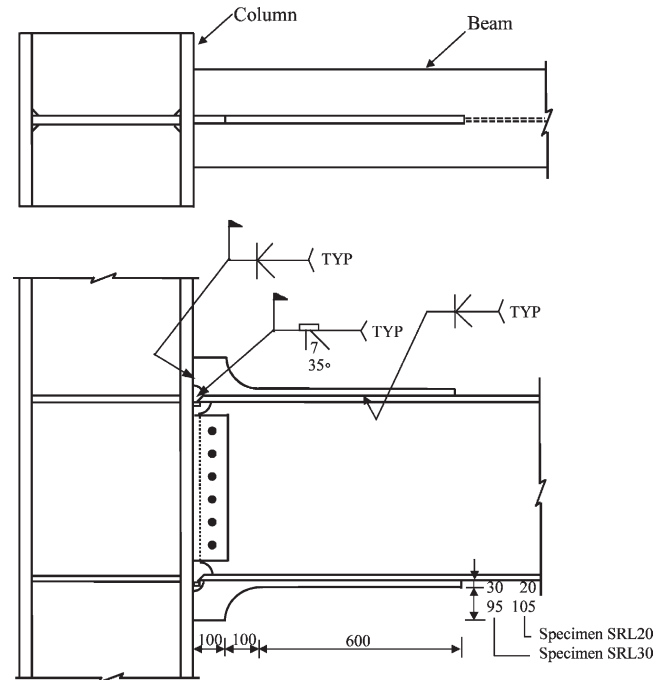


Fig. 4. Connection details of specimens SRL30 and SRL20.

rib extension. The design of the ribs used for the specimens was more conservative than that adopted in the finite element analysis. In regard to the welding procedure, the flange rib was welded first by welding the rib plate to the beam flange along the beam centerline. This welding can be performed in the shop to prevent

Table 2
Mechanical properties of test specimens

Specimen	Coupon location	Yield stress (MPa)	Ultimate stress (MPa)
SRL30	Beam flange	301	437
	Beam web	334	446
	Column flange	401	566
	Column web	374	542
	Rib plate	429	583
SRL20	Beam flange	301	437
	Beam web	334	446
	Column flange	401	552
	Column web	429	583
	Rib plate	397	559

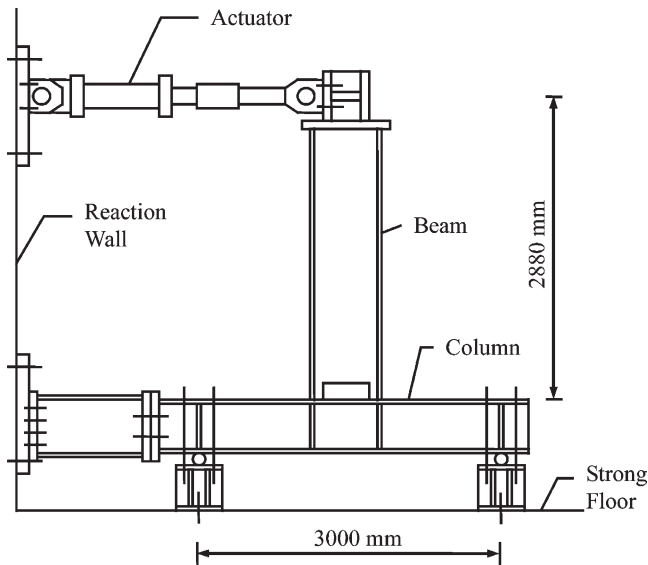


Fig. 5. Schematics of test setup.

an overhead position of the field welding in the bottom flange. The vertical groove weld between the rib and column flange was performed after the complete joint penetration groove weld connecting the beam flange to column flange was completed. Given the reinforcing effect of the rib, backing bars and weld tabs used for groove welding were left in place.

4.2. Test setup and procedure

The test setup, as shown in Fig. 5, simulates the boundary conditions of the subassembly. Cyclic loading was imposed by applying a predetermined cyclic incremental displacement history at the beam tip. The ATC-24 [21] testing protocol shown in Fig. 6 was adopted for this testing history. Imposed displacement

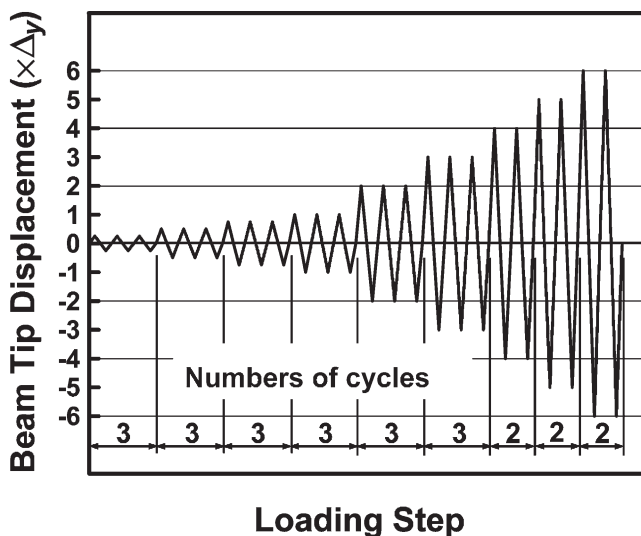


Fig. 6. Loading history.

amplitudes were in multiples of Δ_y , 14.5 mm, which represented a story drift angle of 0.46%. A lateral support near the actuator was provided to prevent lateral deformation of the beam and damage to the actuator. Global deformation of the specimen was measured during the test to determine the beam tip deformation components contributed from column, panel zone, and beam.

5. Results and discussion

5.1. Specimen SRL30

As intended, the specimen initially yielded in the beam flange located at the rib extension. During the cycles of 2.3% story drift, the beam flanges at both ends of the rib extension exhibited minor local buckling. Story drift was calculated by the displacement at the beam tip divided by the length to the centerline of the column. Slight lateral torsional buckling was noticed during the cycles of 2.8% story drift since the lateral restraint was not sufficiently stiff, causing lateral torsional buckling of the beam. Fig. 7 shows the yielding and buckling of the beam at a story drift of 3.2%.

Fig. 8 plots the relationship between the moment and the total plastic rotation. The moment was calculated from the actuator loads multiplying the distance to the column face. The total plastic rotation was computed by subtracting the elastic rotation from the total rotation, i.e., the story drift angle. Strength deterioration revealed in the moment-plastic rotation curves is due to the local buckling of the beam flanges, beam web, and the lateral torsional buckling of the beam. Specimen SRL30 developed a total plastic rotation of 4% radians before the test was terminated because of excessive lateral torsional buckling and significant strength degradation. At the end of the testing, fracture of the rib plate was developed at the front end of the rib extension. At the same location, a small crack was also observed in the weld between the rib plate and the beam flange.

5.2. Specimen SRL20

Stiffer lateral bracing was provided for specimen SRL20 to prevent the effect of lateral torsional buckling of the beam. Specimen SRL20 behaved similarly as specimen SRL30 except that lateral torsional buckling of specimen SRL20 was minor. Fig. 9 shows the extensive yielding in the beam flanges at the cycles of 2.8% story drift. At a story drift of 3.2%, beam flanges local buckling and lateral torsional buckling occurred, causing the strength deteriorated. Fig. 10 shows local buckling of the beam flanges and the beam web in specimen SRL20 at 3.7% drift. Fig. 11 plots beam moment versus total plastic rotation. The hysteretic behaviour of moment-total plastic rotation curve demonstrated that specimen

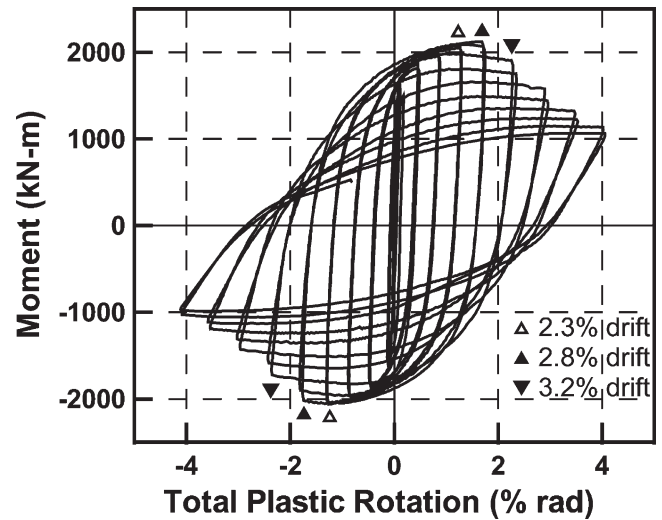


Fig. 8. Specimen SRL30 moment-plastic rotation response.



Fig. 7. Yielding and buckling pattern of specimen SRL30 at 3.2% drift.

SRL20 absorbed a significant amount of the inelastic energy. Specimen SRL20 achieved a total plastic rotation of 4.4% radians while the flexural strength still exceeded the nominal plastic flexural strength of the beam. The final failure was due to a crack occurred at the front end of the rib extension, and the crack penetrated into the beam flange, at a story drift of 5.1%.

When compared with the hysteresis curve of specimen SRL30, hysteresis curve of specimen SRL20 demonstrates gradual deterioration in strength. Lateral torsion buckling of specimen SRL30 occurred at 2.8% drift while that of specimen SRL20, with stiffer bracing, happened at 3.2% drift. As indicated in the moment-plastic rotation curves, shown in Figs. 8 and 11, the strengths of both specimens dropped right after the lateral torsional buckling occurred, and specimen SRL30 showed more



Fig. 9. Formation of beam flange yielding of specimen SRL20 at 2.8% drift.



Fig. 10. Local buckling in specimen SRL20 at 3.7% drift.

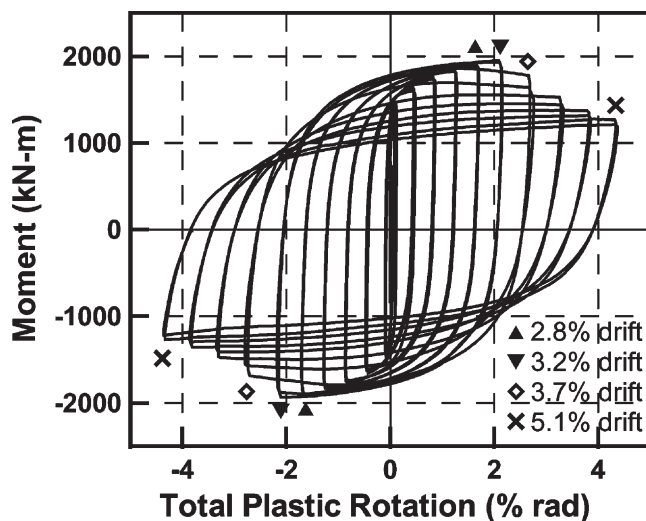


Fig. 11. Specimen SRL20 moment-plastic rotation response.

rapid decrease in strength. Though the lateral torsional buckling amplitude was not measured during the test, lateral deformation could be visualized. It was found that the lateral deformation of specimen SRL30 was much more than that of specimen SRL20 as shown in Figs. 7(a) and 10. However, it should be noted that both specimens exhibited the same degree of deformation of the local buckling in the beam flange and web. The difference of the strength deterioration may be attributed primarily to the stiffness of the lateral bracing since stiffer bracing provides more reliable lateral stability.

5.3. Effectiveness of single lengthened rib

Both specimens exhibited behaviour as observed in the finite element analysis in the way of forming plastic hinge at a distance far from column face and developing much yielding in the beam flange within the rib extension. The test demonstrated the effectiveness of the single lengthened rib. The reinforcement of the rib definitely reduced the stress demand in the beam flange groove weld. No crack was observed in the beam-to-column complete joint penetration groove weld, nor was a through beam flange thickness crack observed at the toe of the weld access hole.

The size of the columns in the specimens resulted in a strong panel zone. Therefore, the panel zone and the column remained elastic throughout the loading history, and the rotation caused by shear deformation of the panel zone was negligible. The plastic rotation of the specimens was fully developed by the beam. Both specimens achieved the plastic rotation of 3% radians required for steel special moment-resisting frames during a cyclic loading test [22].

As demonstrated in the test, the plastic hinge mechanism of the beam formed away from the face of the column. The yielding zone of the beam, located in the rib extension, ensured the development of reliable hysteretic behaviour and the dissipation of energy by the extensive yielding of the beam. Both specimens exhibited reliable plastic rotations and showed no sign of the brittle failure.

5.4. Effect of rib extension

The main difference in the design of specimens SRL30 and SRL20 was the size of the rib extension. Specimen SRL30's rib extension had a 30×30 mm cross section, resulting in a higher plastic modulus than that of specimen SRL20. The ratios of plastic flexural strength of the rib extension to that of the beam section, $Z_{rib}F_{rib}/ZF_y$, were 0.17 and 0.07 for specimens SRL30 and SRL20, respectively. Z_{rib} and Z represent the plastic moduli for the cross sections of the rib extension and the beam, respectively, and F_{rib} and F_y are the measured yield strengths of the rib extension and the beam, respectively. Yielding of the beam began at the front end

Table 3
Flexural strength summary

Specimen	Calculated plastic flexural strength		Maximum test flexural strength		Ratio of test to calculated strength	
	At column face	At plastic hinge	At column face	At plastic hinge	$\frac{M_{pj, test}}{M_{pj}}$	$\frac{M_{ph, test}}{M_{ph}}$
	M_{pj} (kN-m)	M_{ph} (kN-m)	$M_{pj, test}$ (kN-m)	$M_{ph, test}$ (kN-m)		
SRL30	2312	1642	+2122	+1934	0.92	1.18
			−2058	−1915	0.89	1.17
SRL20	2111	1500	+1948	+1813	0.92	1.21
			−1935	−1800	0.92	1.20

of the rib extension at which plastic hinge formed, since the moment gradient of the beam increased linearly from the beam tip. Therefore, specimen SRL30 had a higher maximum test flexural strength than specimen SRL20 since the maximum test flexural strength was controlled by the plastic modulus of the beam with the rib extension.

Table 3 summarizes the flexural strengths at the locations of the column face and the plastic hinge, for both specimens. Calculated plastic flexural strengths were based on the actual yield stress determined in the coupon test. The ratios of the maximum test flexural strength to the calculated plastic flexural strength at the plastic hinge, $M_{ph, test}/M_{ph}$, were in the range of 1.17–1.21, with an average value of 1.19. These ratios clearly indicate that the yielding zone of the beam underwent large inelastic deformation, even in the strain hardening range, when specimens reached their maximum flexural strength. The ratios of the tested to calculated flexural strength at the column face, $M_{pj, test}/M_{pj}$, were only in the range 0.89–0.92. Accordingly, the provided flexural strengths of the beams at the column face exceeded the flexural demand. This result implies that the beams at the column face did not reach the plastic flexural strength and were still elastic, preventing the failure of the joint occurred at the interface of the beam and the column.

The overall length of both lengthened ribs was 800 mm; however, the length of the main reinforced part and the curved part was 200 mm only. The plastic hinge formed right beyond the curved part. Nevertheless, the length of the triangular plate used in the specimens tested by Engelhardt et al. [6] and Anderson and Duan [17] were 559 and 356 mm, respectively. It is apparent that possible plastic hinge location for triangular rib reinforced connection was designed to occur on the beam at the rear end of those ribs. As plastic hinges form at both ends of a beam used in the moment-resisting frame, it is believed that the shorter distance from the column face to plastic hinge, the less flexural demand at the beam-to-column interface. Specimens SRL30 and SRL20 had shorter plastic hinge formation distance from the column face and did not show any damage occurred at the weld between rib plate and the column flange.

Moreover, the purpose of the rib extension is evident that both specimens did not fail by tearing the beam flange.

6. Conclusions

Based on both analytical studies and experimental results, the following conclusions can be drawn concerning moment connections strengthened by the single lengthened rib.

1. A single lengthened rib functions as a reinforcement to prevent brittle fracturing at the beam groove weld. The lengthening of the rib mitigates the stress concentration and prevents the fracture across the beam flange at the rib end.
2. Finite element analysis clearly shows that the single lengthened rib can reduce the local stress concentration at the toe of the weld access hole, and form the desired plastic hinge at the beam section away from the column face.
3. The test results demonstrate that this type of connection exhibits significant, reliable ductility to sustain desired inelastic deformation, and shows no sign of brittle fracture.
4. Specimens developed the required 3% radians of plastic rotation. The column and panel zone remained elastic, and the plastic rotation capacity of the connection was due primarily to the beam.
5. Further study is needed to elucidate the effects of the lengthened rib and determine its dimensions since the conclusions presented here are based on a very limited analytical and experimental study.

Acknowledgements

The authors would like to thank the Sinotech Engineering Consultants, Inc. for financially supporting this research.

References

- [1] SAC Joint Venture. Interim guidelines: evaluation, repair, modification and design of welded steel moment frame structures. Report no. SAC-95-02, FEMA 267, Federal Emergency Management Agency, Washington DC, 1995.
- [2] Miller DK. Lessons learned from the Northridge earthquake. *Engineering Structures* 1998;20(4-6):249–60.
- [3] Nakashima M, Inoue K, Tada M. Classification of damage to steel buildings observed in the 1995 Hyogoken-Nanbu earthquake. *Engineering Structures* 1998;20(4-6):271–81.
- [4] Lin KC, Tsai KC, Kong SL, Hsieh SH. Effects of panel zone deformations on cyclic performance of welded moment connections. In: *Proceedings of the 12th World Conference on Earthquake Engineering*, New Zealand, 2000.
- [5] Engelhardt MD, Sabol TA. Reinforcing of steel moment connections with cover plates: benefits and limitations. *Engineering Structures* 1998;20(4-6):510–20.
- [6] Engelhardt MD, Sabol TA, Aboutaha RS, Frank KH. Testing connections. *Modern Steel Construction*, AISC 1995;35(5):36–44.
- [7] Kim T, Whittaker AS, Gilani AS, Bertero VV, Takhirov SM. Experimental evaluation of plate-reinforced steel moment-resisting connections. *Journal of Structural Engineering*, ASCE 2002;128(4):483–91.
- [8] Uang CM, Yu QS, Noel S, Gross J. Cyclic testing of steel moment connections rehabilitated with RBS or welded haunch. *Journal of Structural Engineering*, ASCE 2000;126(1):57–68.
- [9] Uang CM, Bondad D. Cyclic performance of haunch repaired steel moment connections: experimental testing and analytical modeling. *Engineering Structures* 1998;20(4-6):552–61.
- [10] Yu QS, Uang CM, Gross J. Seismic rehabilitation design of steel moment connection with welded haunch. *Journal of Structural Engineering*, ASCE 2000;126(1):69–78.
- [11] Plumier A. The dogbone: back to the future. *Engineering Journal*, AISC 1997;2nd quarter:61–7.
- [12] Chen SJ, Yeh CH, Chu JM. Ductile steel beam-to-column connections for seismic resistance. *Journal of Structural Engineering*, ASCE 1996;122(11):1292–9.
- [13] Engelhardt MD, Winneberger T, Zekany AJ, Potyraj TJ. Experimental investigation dogbone moment connections. *Engineering Journal*, AISC 1998;4th quarter:128–39.
- [14] Chen SJ, Chu JM, Chou ZL. Dynamic behavior of steel frames with beam flanges shaved around connection. *Journal of Constructional Steel Research* 1997;42(1):49–70.
- [15] Iwankiw NR, Carter CJ. The dogbone: a new idea to chew on. *Modern Steel Construction*, AISC 1996;36:18–23.
- [16] Jones SL, Fry GT, Engelhardt MD. Experimental evaluation of cyclically loaded reduced beam section moment connections. *Journal of Structural Engineering*, ASCE 2002;128(4):441–51.
- [17] Anderson JC, Duan X. Repair/upgrade procedures for welded beam to column connections. Report no. PEER 98/03, Pacific Earthquake Engineering Research Center, Richmond, CA, 1998.
- [18] Zekioglu A, Mozaffarian H, Chang KL, Uang CM, Noel S. Designing after Northridge. *Modern Steel Construction*, AISC 1997;37(3):36–42.
- [19] ANSYS user manual. Swanson Analysis Systems, Inc., 2001.
- [20] AISC. *Manual of steel construction: load and resistance factor design*, 3rd ed. Chicago, IL: American Institute of Steel Construction; 2001.
- [21] ATC. *Guidelines for seismic testing of components of steel structures*. Report ATC-24, Applied Technology Council, Redwood City, CA, 1992.
- [22] AISC. *Seismic provisions for structural steel buildings*. Chicago, IL: American Institute of Steel Construction; 1997.